OAK RIDGE NATIONAL LABORATORY
operated by
UNION CARBIDE CORPORATION • NUCLEAR DIVISION
for the
U.S. ATOMIC ENERGY COMMISSION

ORNL-TM- 3615

DATE - November 1, 1971

Neutron Physics Division

A CALCULATIONAL METHOD FOR PREDICTING PARTICLE SPECTRA FROM HIGH-ENERGY NUCLEON AND PION COLLISIONS ($\geq$ 3 GeV) WITH PROTONS

T. A. Gabriel, R. T. Santoro, J. Barish*

Abstract

A calculational method for predicting the spectra from high-energy nucleon and pion collisions ($\geq$ 3 GeV) with protons is described. The determination of nucleon-proton and pion-proton total, elastic, and nonelastic cross sections from experimental data is discussed, and procedures for obtaining nucleon and charged-pion spectra from the Ranft-Borak distributions are presented. A brief discussion of the computer program logic is also included.

*Mathematics Division

NOTE:
This Work Partially Funded by
NATIONAL AERONAUTICS AND SPACE ADMINISTRATION
Under Order H-38280A

I. INTRODUCTION

A calculational method for treating the individual collisions of high-energy ($\geq$ 3 GeV) nucleons and charged pions with protons has been adapted to the high-energy nucleon-meson transport code HETC.[1] This method provides detailed information on both elastic and nonelastic nucleon- and charged-pion-proton collisions.

Previously, high-energy distributions were estimated in HETC using a nucleon- and pion-nucleon scaling model[2] that related the collision data at 3 GeV to higher energies. This method, however, was not entirely successful in predicting the high-energy particle distributions. The method of calculation and the procedures described here have now been incorporated into HETC, and the accuracy of the code has been increased.

The determination of nucleon-proton and pion-proton cross sections and methods for obtaining differential cross sections are presented in the sections to follow. A brief discussion and a flow diagram of the procedure for calculating the nonelastic differential cross section are also given.

II. ANALYTICAL METHODS

A. Nucleon-Proton and Pion-Proton Total, Elastic, and Nonelastic Cross Sections

The nucleon-proton and charged-pion-proton interaction cross sections for nucleon and pion energies $\geq$ 3 GeV were obtained from the compilations of Barashenkov[3] and Bertini et al.[4,5] Inclusion of these data into the calculational method was accomplished using parametric fitting techniques to obtain analytic functions. These functions represent reasonable estimates of the cross sections with regard to experimental data even though an error analysis, such as a least-squares fit, has not been made. The total, elastic, and nonelastic cross sections for p + p, n + p, π^+ + p, and π^- + p collisions are summarized in Figs. 1-4. The bold lines were obtained using the equations discussed below and the data points were taken from data reported in refs. 3 and 4.

In the following equations the units for the cross sections σ are millibarns and those for the energy E are GeV. For all interactions, the nonelastic cross section is obtained from the difference between the total and elastic cross sections; i.e., $\sigma_{nonel} = \sigma_T - \sigma_{el}$.

<u>p - p collisions</u>

$$\sigma_T = 37.5 + 7.0E^{-0.50} \qquad E \geq 3.5 \text{ GeV}$$

$$\sigma_{el} = 7.0 + 21.03E^{-0.873} \qquad E \geq 3.5 \text{ GeV}$$

<u>n - p collisions</u>

$$\sigma_T = \begin{cases} 42.0 & 3.5 \leq E \leq 8 \text{ GeV} \\ 37.5 + 26.45E^{-0.852} & E > 8 \text{ GeV} \end{cases}$$

$$\sigma_{el} = \begin{cases} -0.222E + 12.48 & 3.5 \leq E \leq 8 \text{ GeV} \\ 6.0 + 73.144E^{-1.32} & E > 8 \text{ GeV} \end{cases}$$

<u>π^+ - p collisions</u>

$$\sigma_T = \begin{cases} -4.66E + 42.95 & 2.5 \leq E \leq 3 \text{ GeV} \\ -0.757E + 31.24 & 3 < E \leq 6 \text{ GeV} \\ 21.5 + 18.91E^{-0.716} & E > 6 \text{ GeV} \end{cases}$$

$$\sigma_{el} = \begin{cases} -1.40E + 10.0 & 2.5 \leq E \leq 3 \text{ GeV} \\ -0.166E + 6.298 & 3 < E \leq 6 \text{ GeV} \\ 3.5 + 9.93E^{-0.953} & E > 6 \text{ GeV} \end{cases}$$

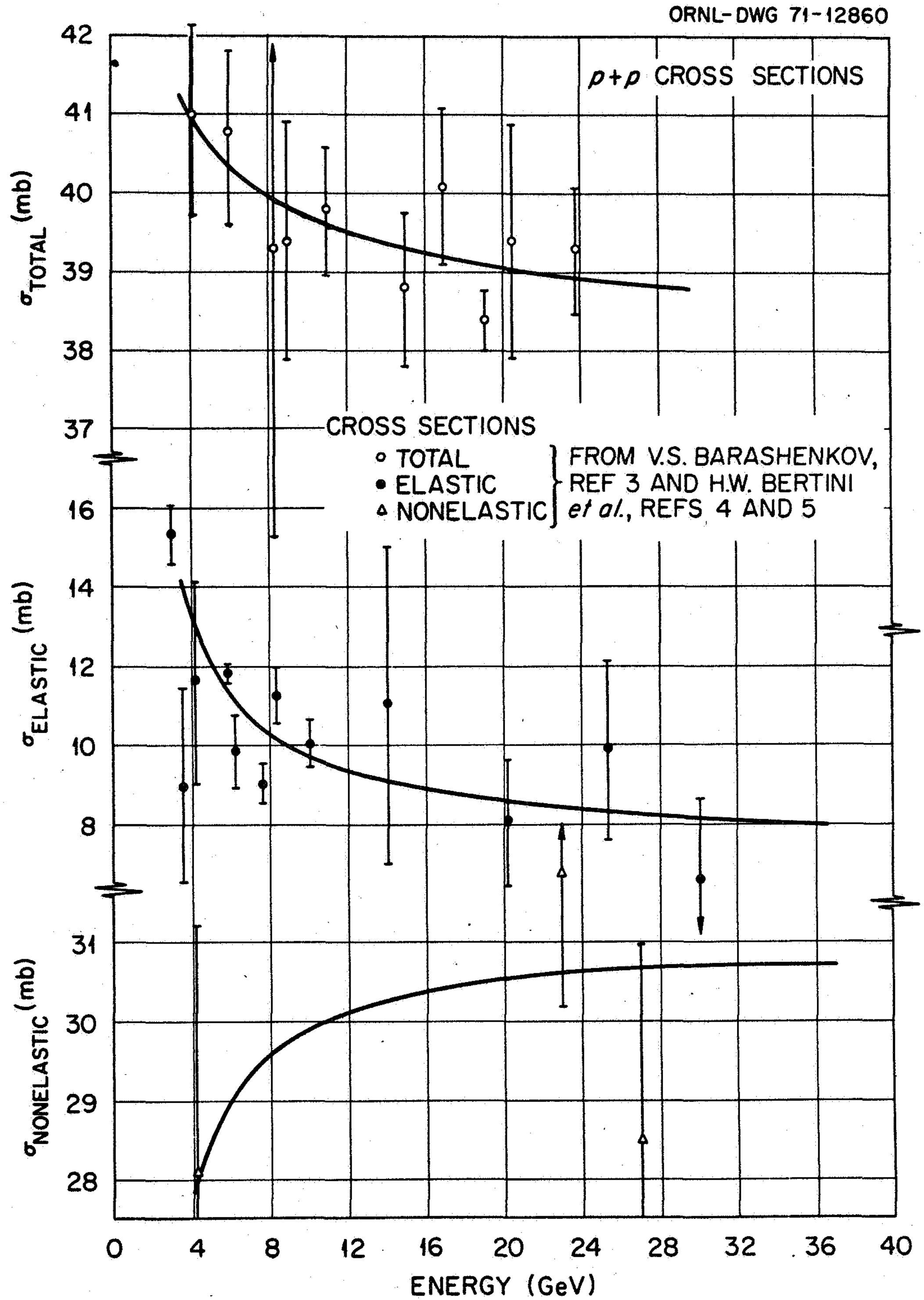

Fig. 1. Total, Elastic, and Nonelastic Cross Sections for p + p Collisions.

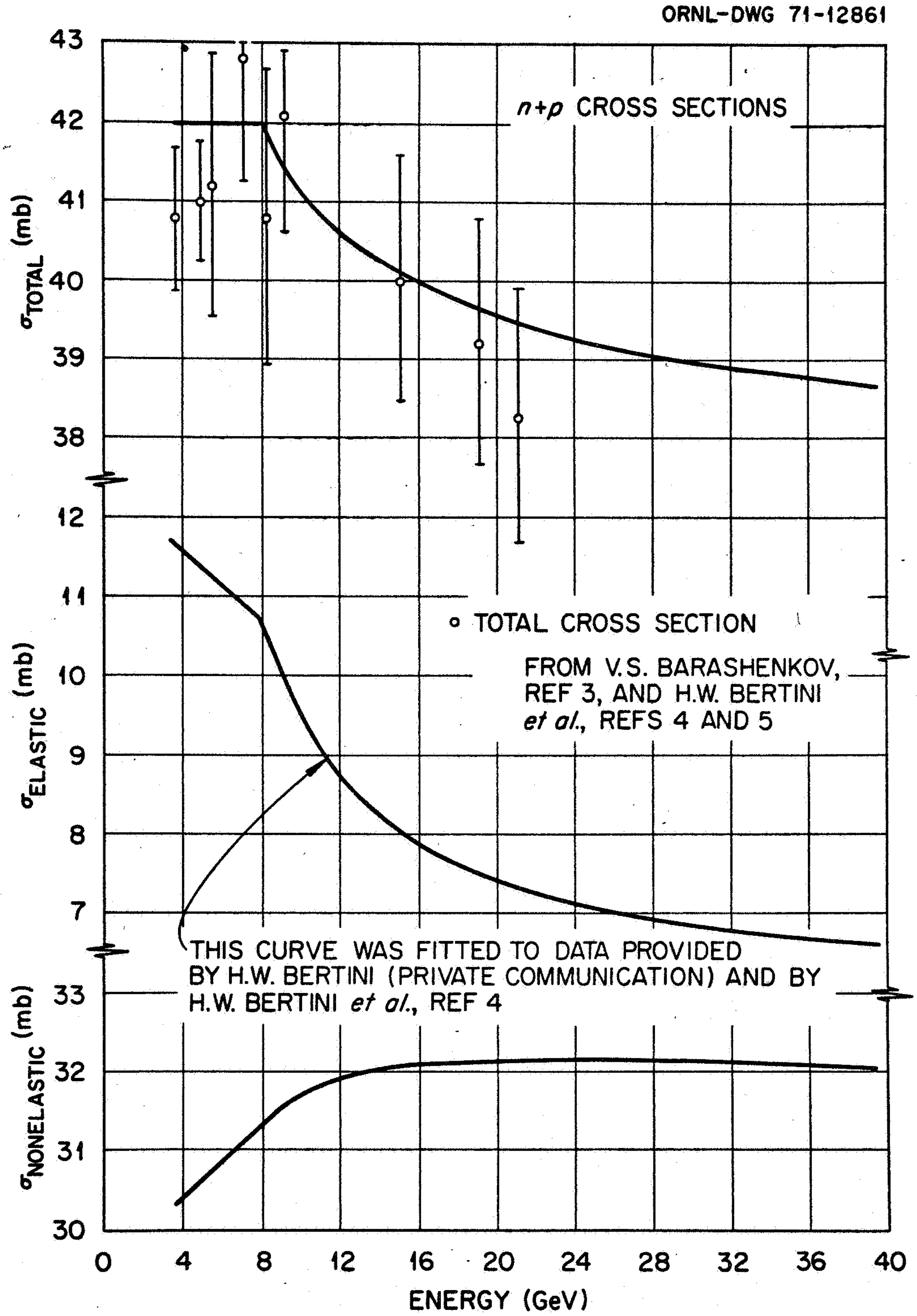

Fig. 2. Total, Elastic, and Nonelastic Cross Sections for n + p Collisions.

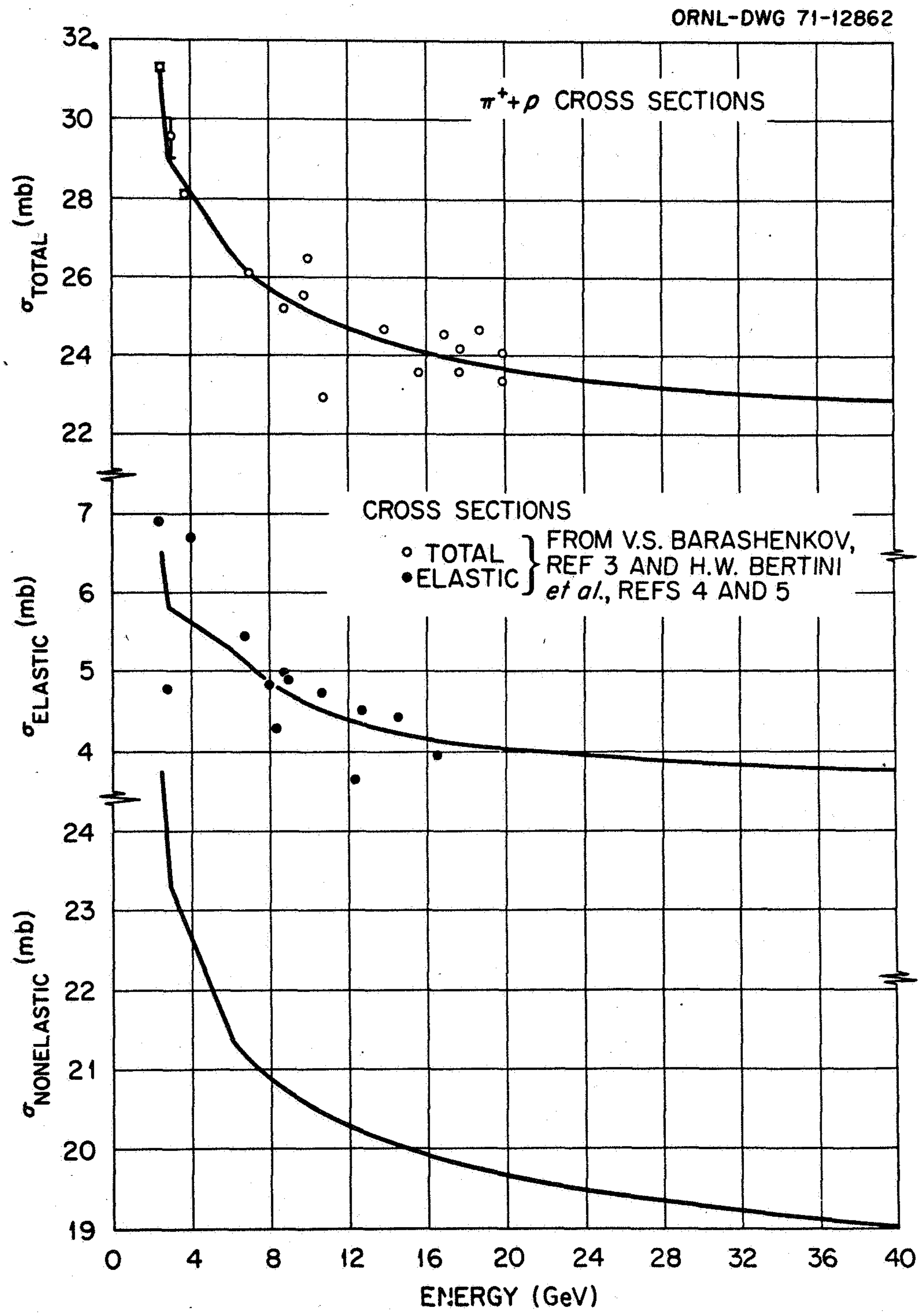

Fig. 3. Total, Elastic, and Nonelastic Cross Sections for $\pi^+ + p$ Collisions.

ORNL-DWG 71-12863

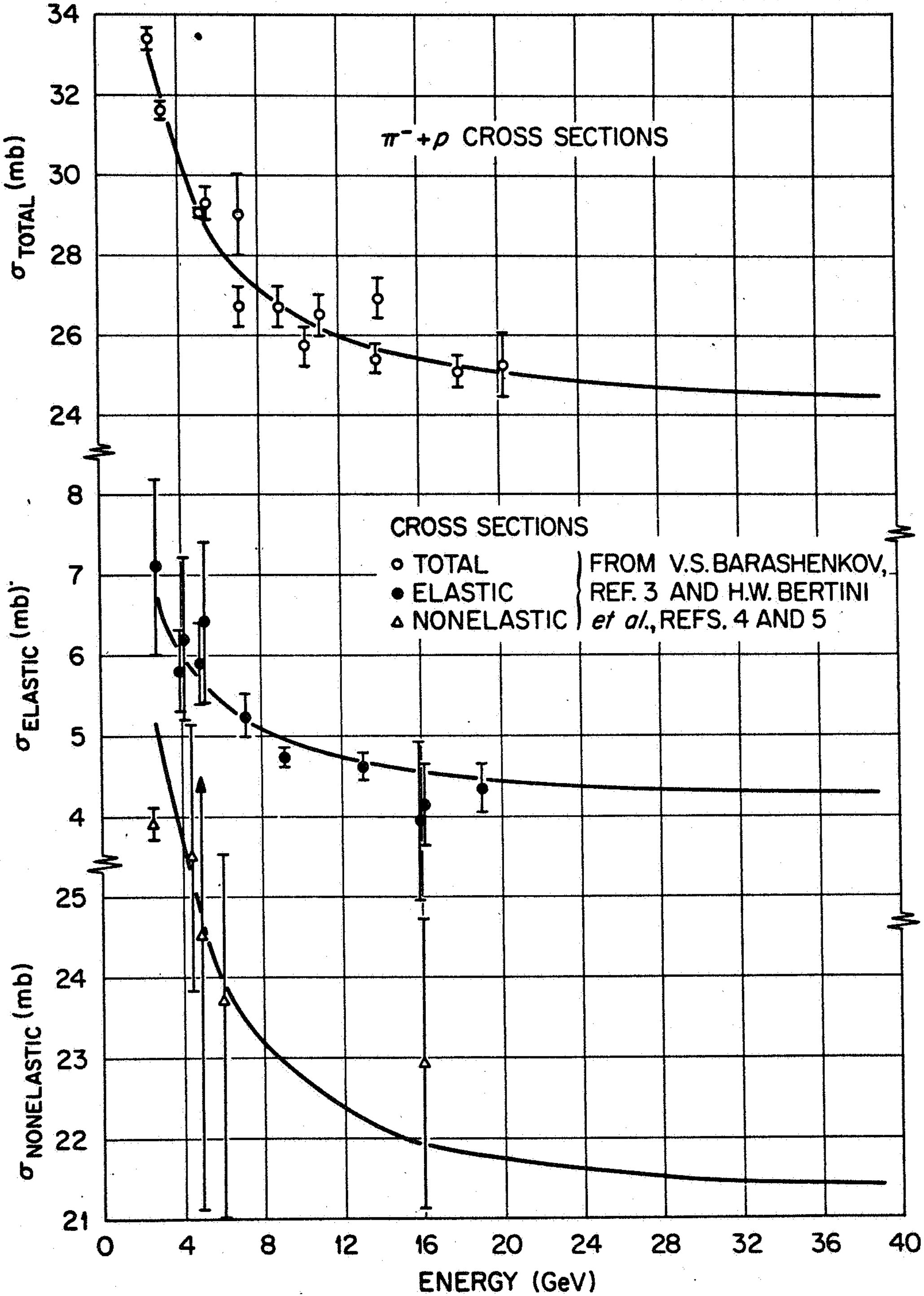

Fig. 4. Total, Elastic, and Nonelastic Cross Sections for π^- + p Collisions.

$\pi^- - p$ collisions

$$\sigma_T = \begin{cases} -1.66E + 37.34 & 2.5 \leq E \leq 5 \text{ GeV} \\ 23.60 + 25.51E^{-0.959} & E > 5 \text{ GeV} \end{cases}$$

$$\sigma_{el} = 3.8 + 7.273E^{-0.896} \qquad E \geq 2.5 \text{ GeV}$$

B. Elastic Nucleon-Proton and Pion-Proton Differential Scattering Cross Sections

The analytic functions for describing the elastic differential cross sections were obtained from parametric fits to experimental data.[5] The fitting equations for describing the elastic differential scattering cross sections for nucleon and pion energies ≥ 3 GeV were obtained from the 4-momenta relation

$$\frac{d\sigma}{dt} = \exp(A + Bt), \tag{1}$$

where t is related to the center-of-mass scattering angle by

$$\cos\theta_{c.m.} = 1 - \frac{|t|}{2K^2}$$

where

$$K^2 = \frac{M^4 - 2M^2(m_1^2 + m_2^2) + (m_1^2 - m_2^2)^2}{4M^2} .$$

In this equation, M is the total energy in the center-of-mass sytem and m_1 and m_2 are the masses of the particles undergoing the elastic collision.

In fitting the parametric equations to the experimental elastic differential cross sections, the following values for B in units of $(\text{GeV}/c)^{-2}$ were used for the indicated reactions

$$B = \begin{cases} 7.26 + 0.0313P_o & \binom{p}{n} + p \\ 7.575 & \pi^- + p \\ 7.040 & \pi^+ + p \end{cases} , \tag{2}$$

where P_o is the incident particle momentum in GeV/c. Figure 5 compares B obtained using Eq. 2 with experimental values of B obtained by Gibbard et al.[6] for p + p and n + p collisions.

In Eq. 1, A is a normalization constant, the magnitude of which is not essential to the determination of the center-of-mass scattering angle.

The cosine of the center-of-mass scattering angle was determined by random sampling through the expression

$$\cos \theta_{c.m.} = 1 + (2K^2B)^{-1} \ln\{1 - R[1 - \exp(-2K^2B)]\}$$

where R is a random number between 0 and 1. Assuming a uniform distribution in the azimuthal scattering angle of the collision products and using the transformations from the center of mass to the laboratory system, the number of particles scattered at an angle θ_{lab} vs the scattering angle θ_{lab} can be obtained. The probability per steradian predicted at the selected angle of scatter for incident 3.5-GeV neutrons vs the cosine of the scattering angle is shown in Fig. 6. The histogram is taken from experimental data cited in ref. 4 and is normalized to the calculated data. The scatter observed in the calculated data arises from statistical variations.

C. Nonelastic Nucleon-Proton and Pion-Proton Collisions

Up to the present time, the best data available for predicting p + p nonelastic events at high energies ($\gtrsim$ 10-20 GeV) have been the analytic fits of Ranft and Borak.[7] These fits, obtained from available experimental data, provide fairly reliable estimates of the double differential cross sections for the production of nucleons and pions from 10- to 20-GeV p + p collisions. No provision is made, however, for estimating the production of nucleons and pions from charged-pion-proton reactions. In the

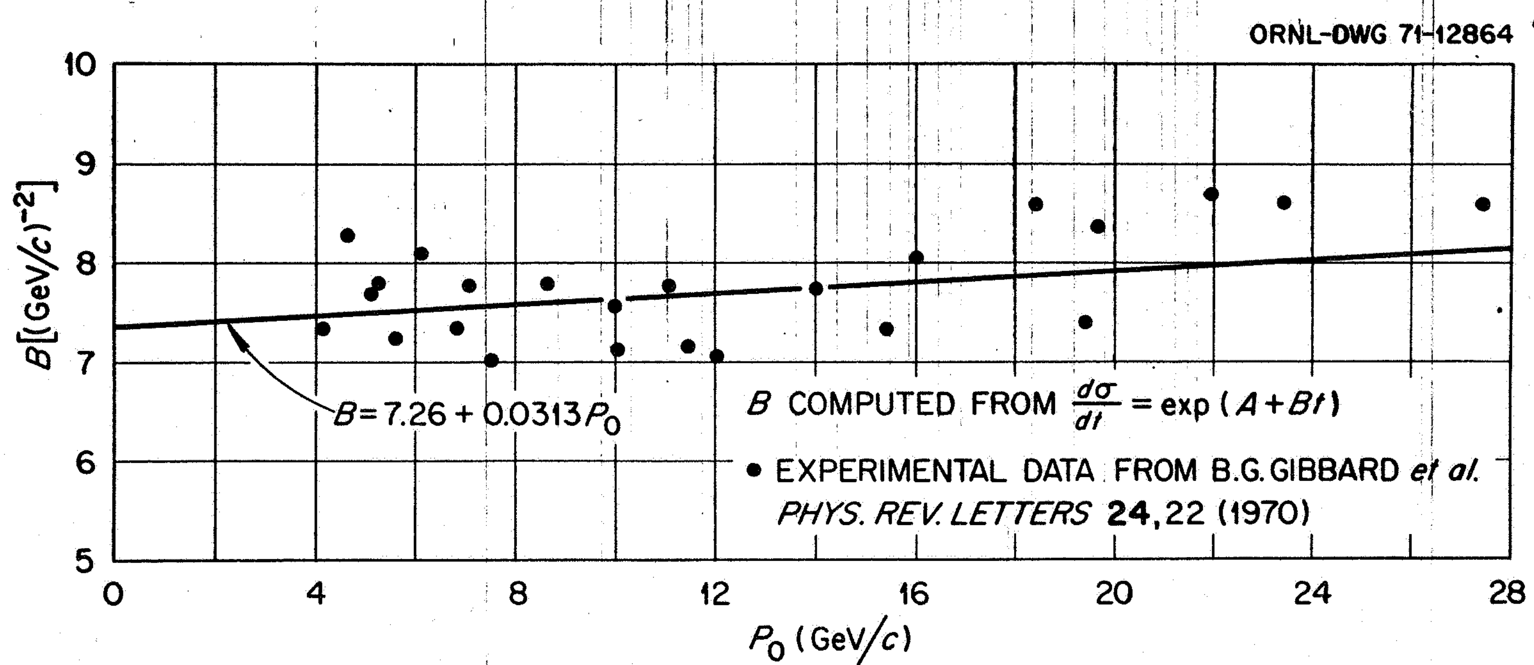

Fig. 5. Variation of the Elastic Scattering Parameter B as a Function of Incident Particle Momentum, P_o.

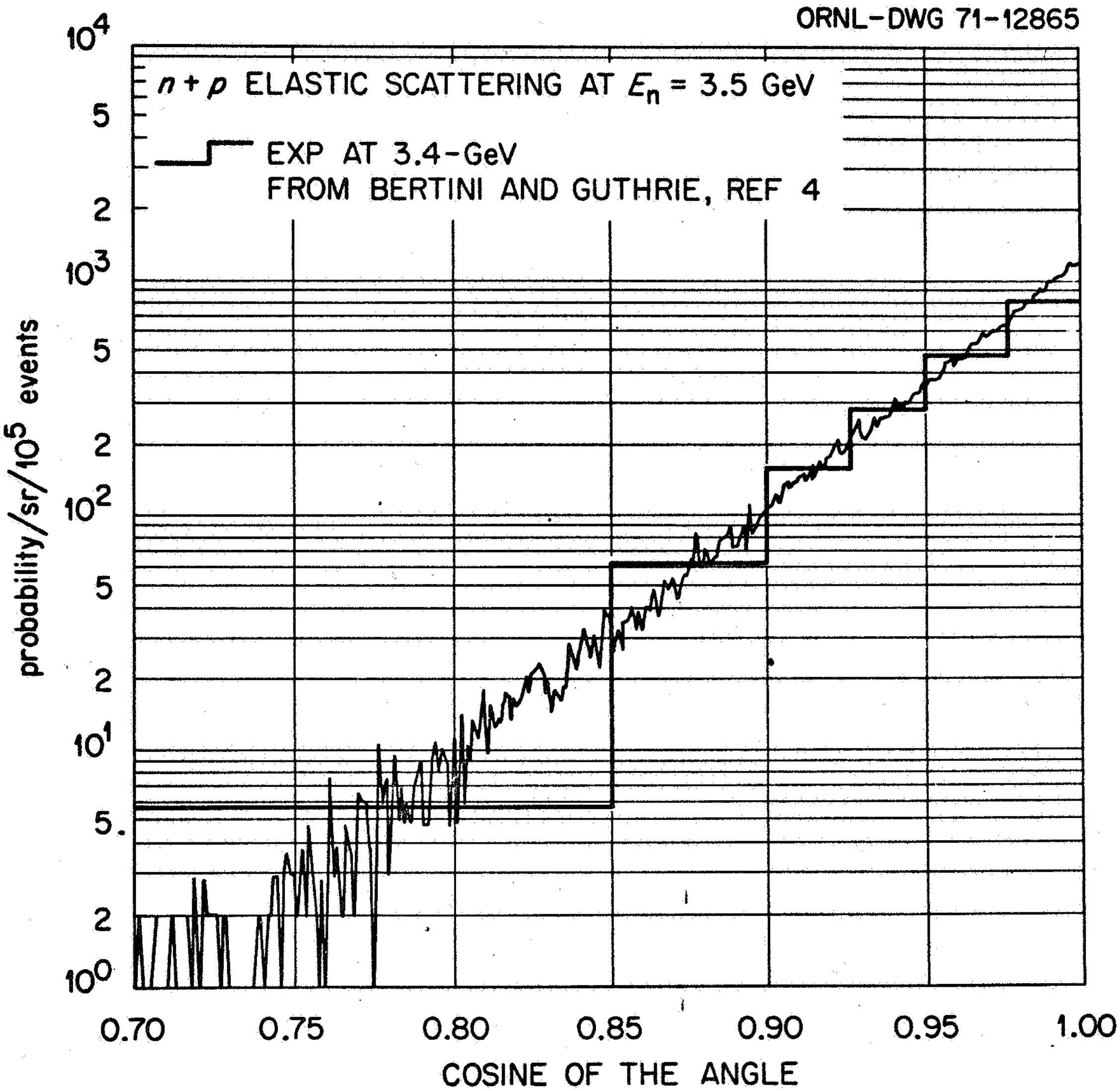

Fig. 6. Probability Per Steradian vs the Cosine of the Scattering Angle.

calculational method described here, the analytic fits obtained by Ranft and Borak have been adapted to estimate nucleon and pion production from proton-, neutron-, and charged-pion-proton collisions.

For each collision event and for the average of many events, energy and nucleons are conserved, and a reproduction of the spectral shape is preserved over an angular interval from 0 to 45°. Standard sampling and storage techniques that can be employed to conserve these quantities are utilized to obtain the secondary particle type, energy, and direction cosines that result from a specified collision.

The spectra of secondary protons from p + p nonelastic collisions are given by Ranft and Borak using the relation[7]

$$\left.\frac{d^2N}{dP\,d\Omega}\right|^{R}_{prot} = \left[\frac{A_1}{P_o} + \frac{A_2 P}{P_o^2}\right]\left[1 + \sqrt{1 + \left(\frac{P_o}{m_p}\right)^2} - \frac{P_o}{P}\sqrt{1 + \left(\frac{P}{m_p}\right)^2}\right]$$

$$\times\ P^2 \times \left[1 + \sqrt{1 + \left(\frac{P_o}{m_p}\right)^2} - \frac{P_o P}{m_p^2\sqrt{1 + \left(\frac{P^2}{m_p}\right)}}\right]\exp(-\,A_3 P^2 \theta^2)\,, \qquad (3)$$

where

P_o = incident nucleon momentum (GeV/c)

P = emitted nucleon momentum (GeV/c)

m_p = proton rest energy (GeV)

θ = angle of emission of secondary nucleons (rad)

A_i; i = 1, 2, 3 constants which define the target particle.

For protons, $A_1 = 0.885$

$A_2 = 0.101$

$A_3 = 4.256$.

Charged-pion production from p + p collisions is given by the Ranft-Borak distributions through the formula

$$\left.\frac{d^2N}{dPd\Omega}\right|^{R}_{\pi^\pm} = A_1P^2 \exp\left[-A_2 \frac{P}{\sqrt{P_o}} - A_3P\sqrt{P_o}\,\theta^2\right] + A_4 \frac{P^2}{P_o} \exp\left[-A_5\left(\frac{P}{P_o}\right)^2 - A_6P\theta\right] , \tag{4}$$

where P and P_o are the momenta of the emitted charged pion and incident nucleon, respectively. The coefficients A_i, i = 1-6, are

	A_1	A_2	A_3	A_4	A_5	A_6
π^+	3.386	4.146	4.556	7.141	9.60	4.823
π^-	3.386	4.146	4.556	1.853	9.60	4.823

In using the distributions given by Eqs. 3 and 4, several assumptions were made independently of the incident particle type. It was assumed that sinθdθ could be approximated by θdθ when the equations were integrated over the angular interval to 45°. Particles at angles wider than 45° were taken to be isotropic with ∿ 3% of all particles allowed to be emitted at these wider angles and with the added restriction that these particles carry no more than 10% of the incident particle energy. Further assumptions attendant to nucleon and pion productions are summarized as follows:

<u>p + p collisions</u>

The double-differential cross sections and particle multiplicities for secondary protons and charged pions are obtained directly from Eqs. 3 and 4. The distribution of secondary neutrons produced in p - p collisions is given by[8]

$$\left.\frac{d^2N}{dPd\Omega}\right|_{neut} = \frac{2 - \nu_{prot}}{\nu_{prot}} \left.\frac{d^2N}{dPd\Omega}\right|^R_{prot} ,$$

when $d^2N/dPd\Omega|^R_{prot}$ is given by Eq. 3. The proton multiplicity, ν_{prot}, is obtained from $\nu_{prot} = \iint(d^2N/dPd\Omega|_{prot})dPd\Omega$. For π_o production, the distribution is given by

$$\left.\frac{d^2N}{dPd\Omega}\right|_{\pi^o} = \frac{\nu_{\pi^o}}{\nu_{\pi^+}} \left.\frac{d^2N}{dPd\Omega}\right|^R_{\pi^+}$$

where $(d^2N/dPd\Omega)|^R_{\pi^+}$ is given by Eq. 4. ν_{π^o} is the π^o multiplicity determined from energy conservation. It was observed that ν_{π^o} goes negative at $\sim$ 14 GeV. Therefore, the energy imparted to nucleons according to the Ranft-Borak distributions at each energy was linearly reduced from 100% at 18 GeV to 75% at 3 GeV for p + p- and n + p-type collisions.

The secondary proton spectra from 3-GeV p + p collisions predicted by the Lindenbaum-Sternheimer isobar model[9] are compared in Fig. 7 with the results obtained using this method. The data are for secondary protons emitted into the angular interval from 5° to 17.5°. The valley in the Lindenbaum-Sternheimer distribution at $\sim$ 1200 MeV/c arises from the angular distribution for particle production imposed in the calculation leading to these data. Comparison of experimentally obtained results with the distribution predicted by the isobar model shows reasonable agreement. The results obtained using the method described here are at best favorable.

π^+ spectra obtained using this method (but not shown here) are in good agreement with the Lindenbaum-Sternheimer results. However, for π^- and π^o spectra the results are less favorable. The π^- spectra are overestimated and the π^o spectra are underestimated.

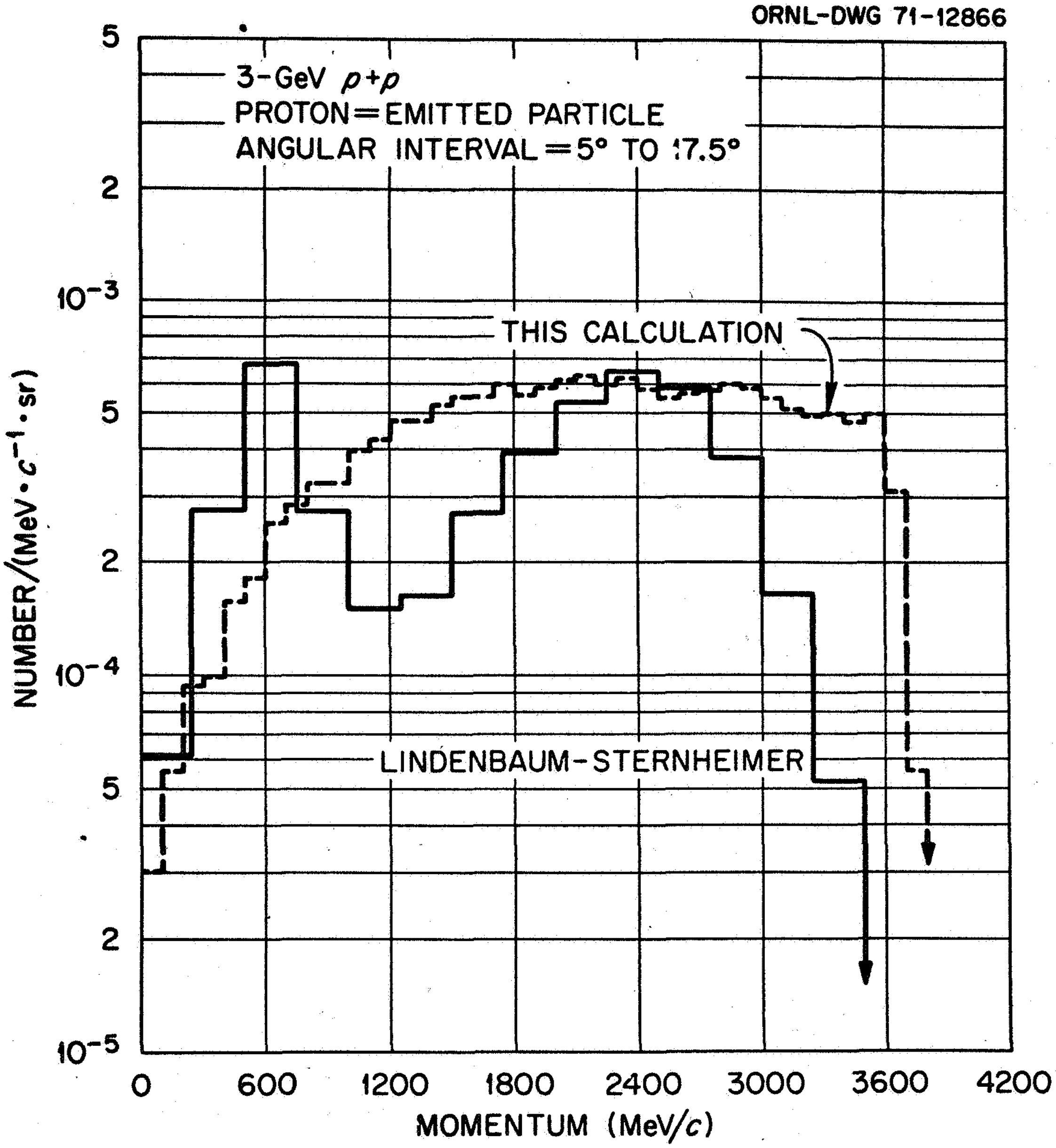

Fig. 7. Secondary Proton Spectra From 3-GeV p + p Collisions.

n + p collisions

For n + p collisions, the proton and neutron multiplicities were taken to be the same; i.e., $\nu_{prot} = \nu_{neut} = 1$. The secondary nucleon distributions were then obtained using

$$\left.\frac{d^2N}{dPd\Omega}\right|_{neut} = \left.\frac{d^2N}{dPd\Omega}\right|_{prot} = \frac{1}{\nu_p}\left.\frac{d^2N}{dPd\Omega}\right|^{R}_{prot} .$$

The secondary charged- and neutral-pion distributions were obtained in the same manner as for p + p collisions. The secondary neutron spectra from 3-GeV n + p collisions obtained using the Lindenbaum-Sternheimer isobar calculation and this method are compared in Fig. 8. The agreement between the data is acceptable for the lower energy limit at which the equations will be applied.

π^+ + p collisions

For π^+ + p collisions, the secondary particle distributions are given by

$$\left.\frac{d^2N}{dPd\Omega}\right|_{\pi^+} = \frac{1 + \nu_{\pi^+}}{\nu_{\pi^+}}\left.\frac{d^2N}{dPd\Omega}\right|^{R}_{\pi^+}$$

and (5)

$$\left.\frac{d^2N}{dPd\Omega}\right|_{prot\ or\ neut} = \frac{0.5}{\nu_{\pi^+}}\left.\frac{d^2N}{dPd\Omega}\right|^{R}_{\pi^+} ,$$

where the proton and neutron multiplicities are given by $\nu_{prot} = \nu_{neut} = \frac{1}{2}$. In these equations, the appropriate rest mass values must be included in the calculation of the incident π^+ momentum and the secondary nucleon momentum.

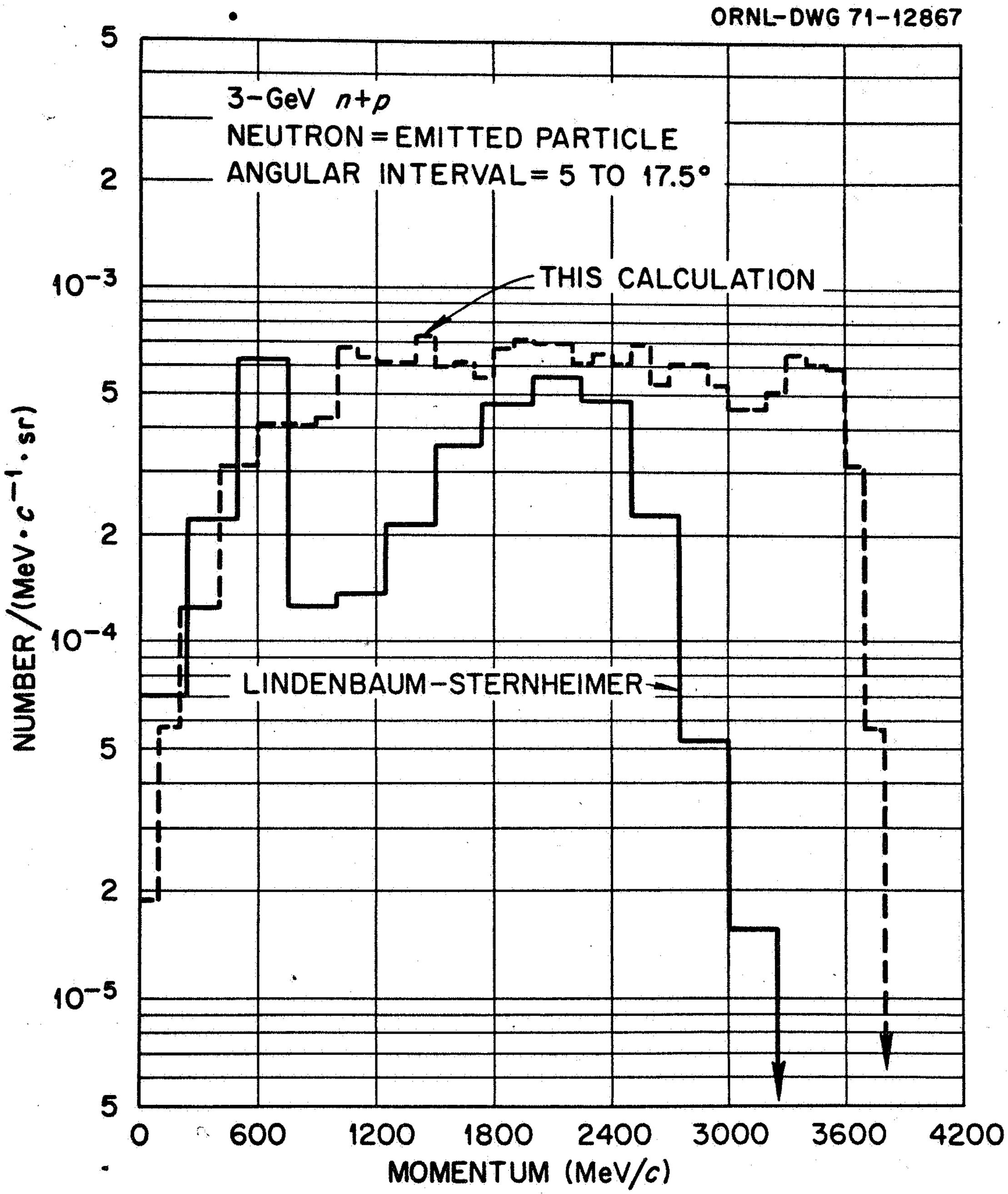

Fig. 8. Secondary Neutron Spectra From 3-GeV n + p Collisions.

Secondary π^--meson spectra are obtained directly from Eq. 4. The π^o spectra were obtained using

$$\left.\frac{d^2N}{dPd\Omega}\right|_{\pi^o} = \frac{\nu_{\pi^o}}{\nu_{\pi^+}} \left.\frac{d^2N}{dPd\Omega}\right|^{R}_{\pi^+}$$

where, as before, ν_{π^o}, the π^o multiplicity is derived from energy conservation.

The π^+ spectrum from $\pi^+ + p$ collisions at 2.5 GeV is compared in Fig. 9 with the spectrum given by Lindenbaum and Sternheimer. The agreement of the data for emitted π^+ at 2.5 GeV is rather poor, although not entirely unexpected. The present method severely overestimates the pion production at this energy and angular interval.

π^- + p collisions

The secondary particle distributions for these reactions are obtained using expressions of the form given for $\pi^+ + p$ collisions with the signs of the charged pions appropriately reversed in Eq. 5. The production of π^+-mesons is given by Eq. 4. Typical results are given in Fig. 10. The agreement is also not favorable for these data.

Comparisons at Higher Energies

Particle spectra predicted by this method at energies of $\sim$ 3 GeV are not in particularly good agreement with the results predicted by Lindenbaum and Sternheimer. However, as the reaction energy increases, the Ranft-Borak distributions more accurately reproduce experimental results for p + p collisions. Comparison between the analytic fits of Ranft and Borak and the proton spectrum predicted by this calculation is shown in Fig. 11 for p + p collisions at 50 GeV. The angular interval over which the Ranft-Borak distributions are averaged is 0 to 10 mrad. The dispersion in the

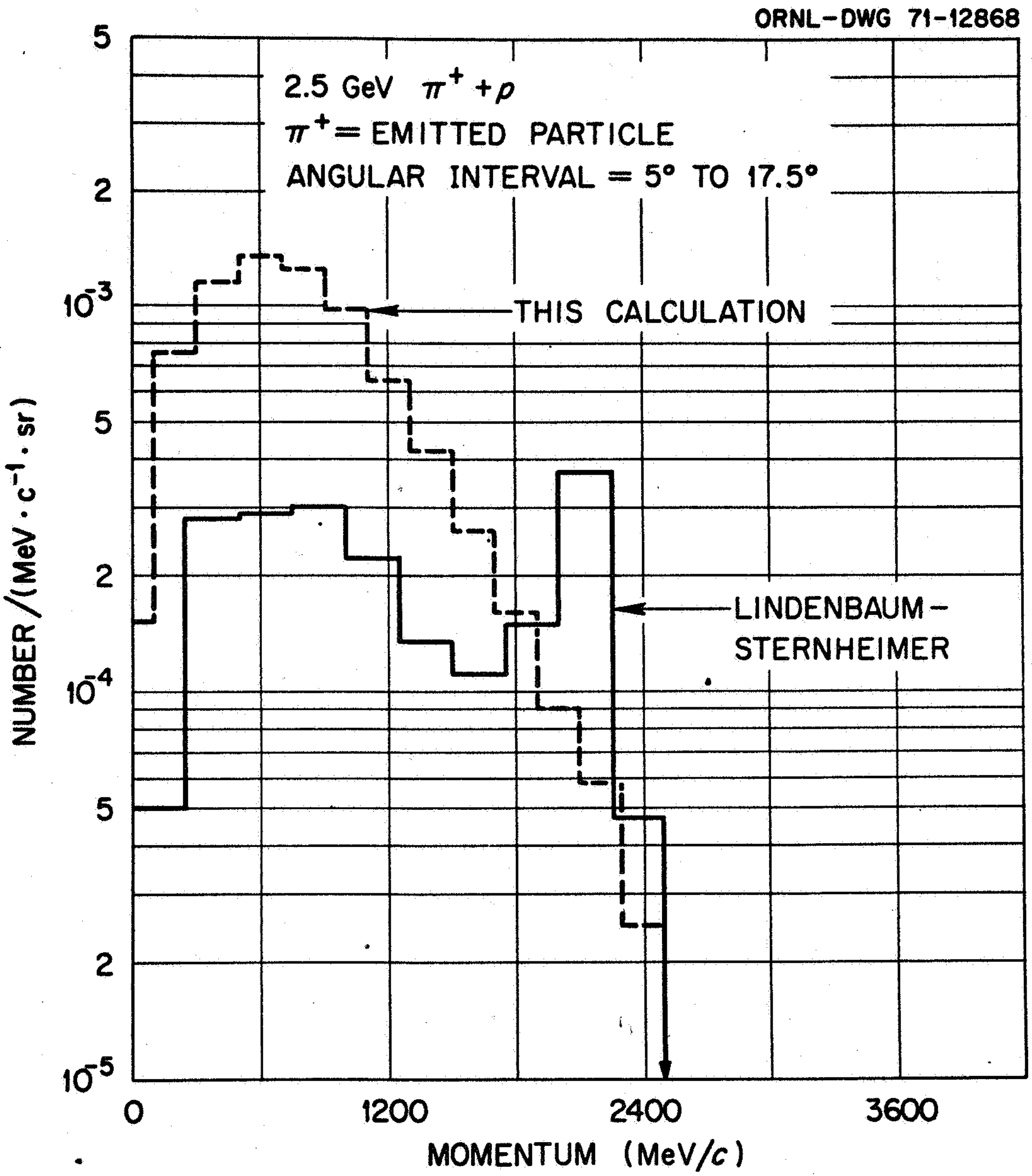

Fig. 9. Secondary π^+ Spectra From 2.5-GeV π^+ + p Collisions.

ORNL-DWG 71-12869

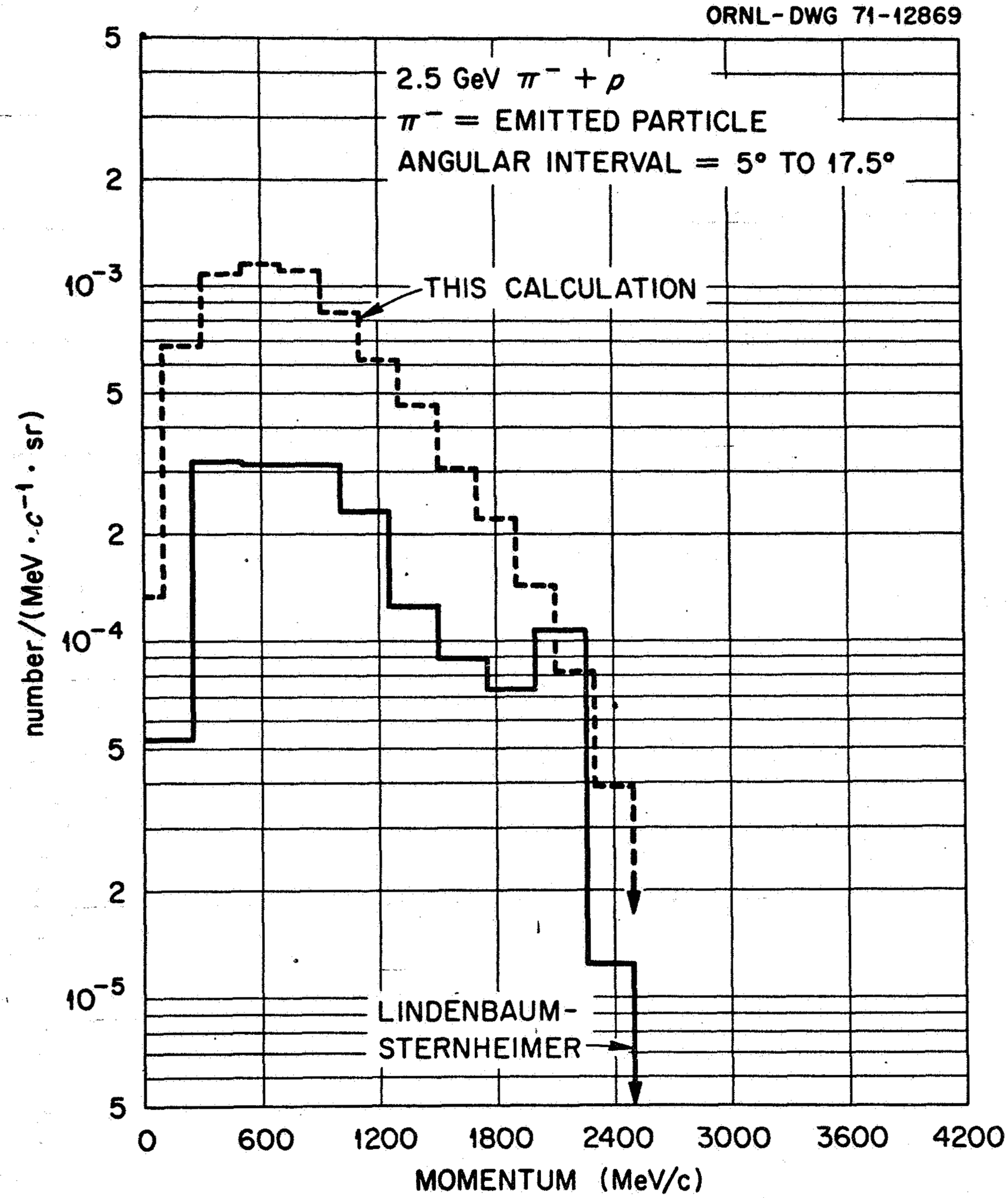

Fig. 10. Secondary π^- Spectra From 2.5-GeV π^- + p Collisions.

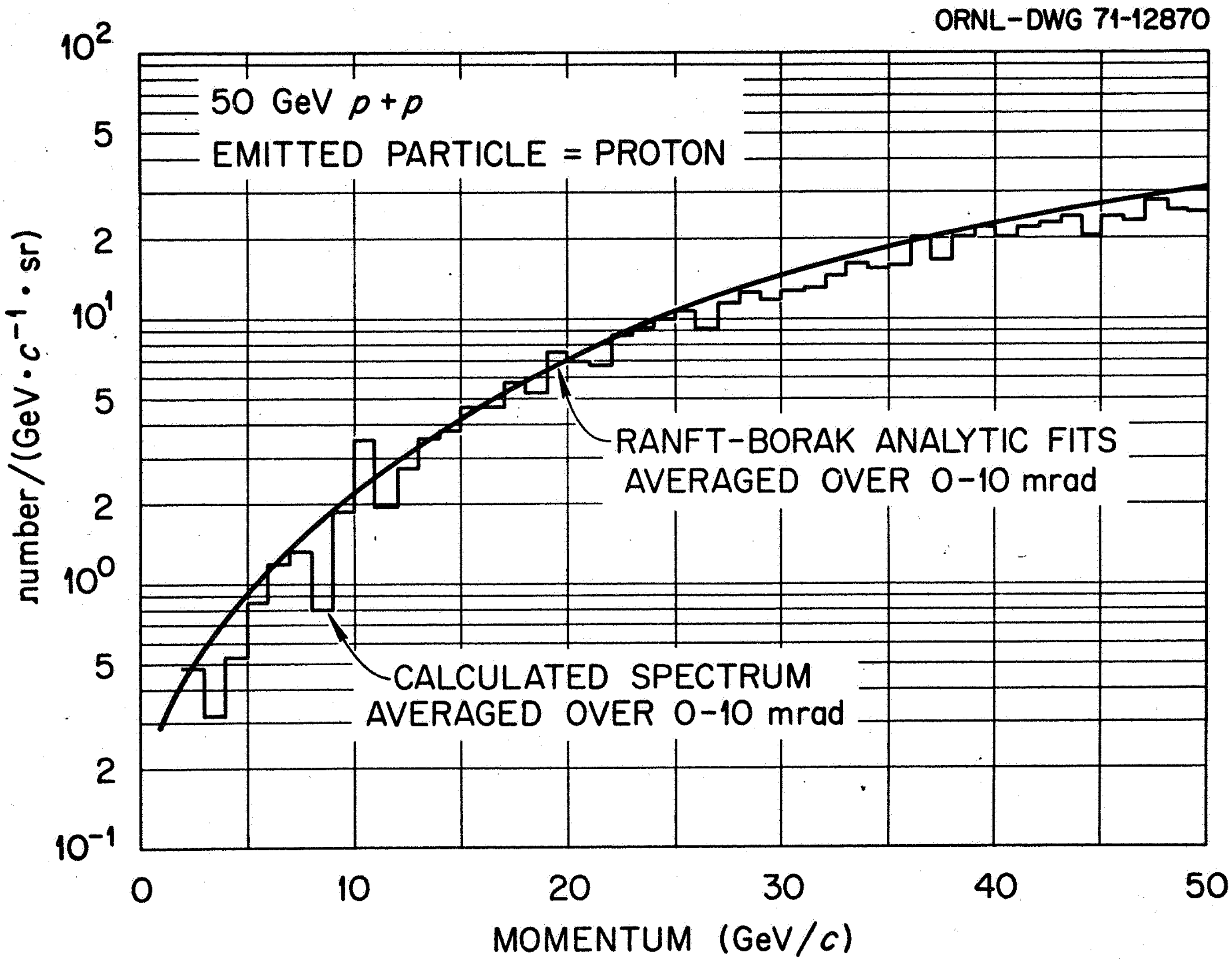

Fig. 11. Proton Spectra From 50-GeV p + p Collisions Averaged Over the Angular Interval From 0 to 10 mrad.

histogram data is from statistical variations. Similar results are shown in Fig. 12 for the π^+ spectra from 50-GeV p + p collisions.

III. CALCULATIONAL PROCEDURES FOR OBTAINING NONELASTIC DIFFERENTIAL CROSS SECTIONS

Figure 13 is a schematic diagram of the sampling and storage procedures used to obtain the nucleon and pion distributions described here. Entry into the package is through calling arguments in HETC.[1]

Each entry into the program package sets up tables of the particle multiplicity from which the particle type is selected. If the particle is not used, or if there is an excess of particles from particle conservation, it is stored in a (primary) table which may be referred to in subsequent entries into the program. The remaining parts of the program are accounting procedures for assuring nucleon and energy conservation.

It should be noted that the calculational procedure will work above 1 TeV. However, the storage tables do not store secondary particles produced by incident particles with energy > 1 TeV.

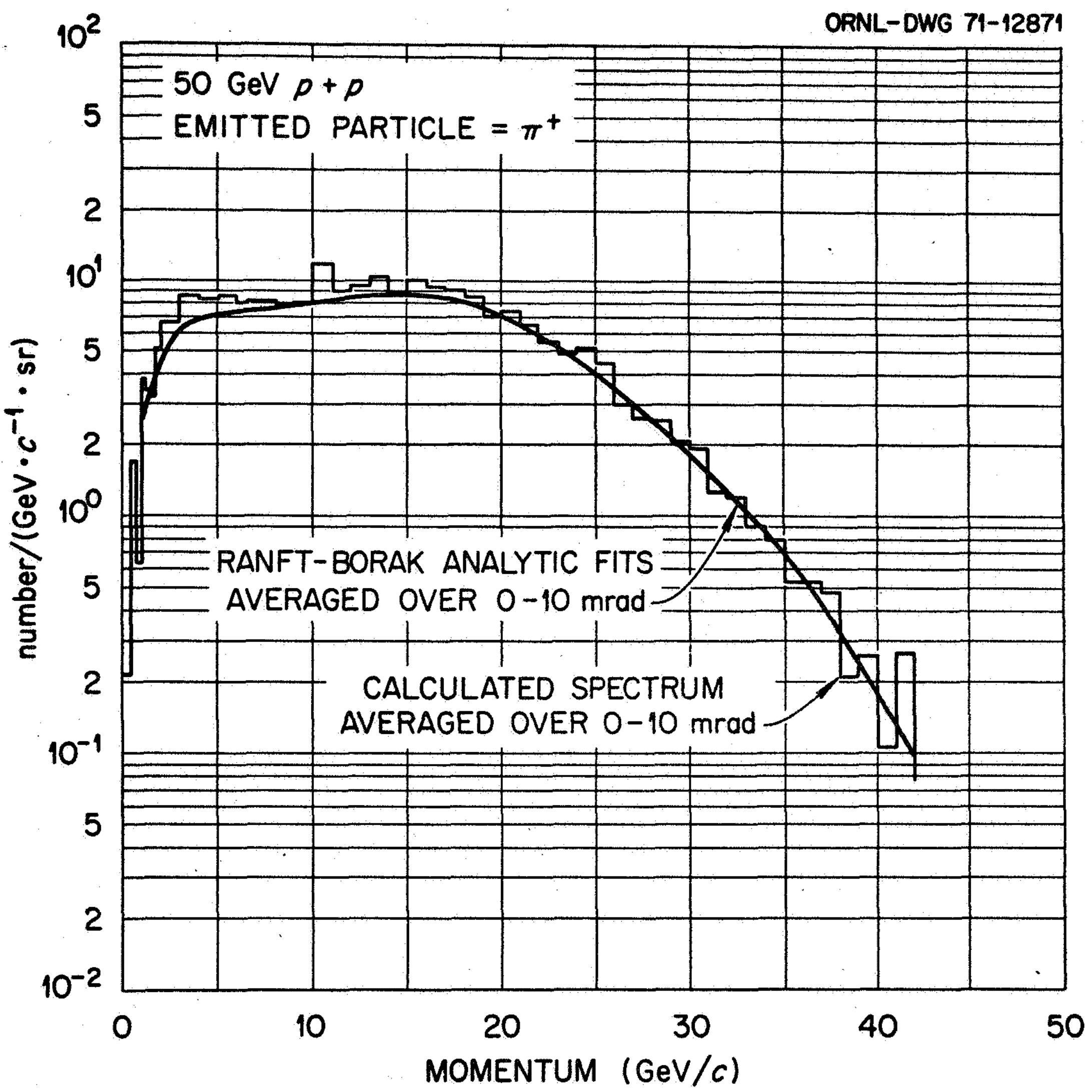

Fig. 12. π^+ Spectra From 50-GeV p + p Collisions Averaged Over the Angular Interval From 0 to 10 mrad.

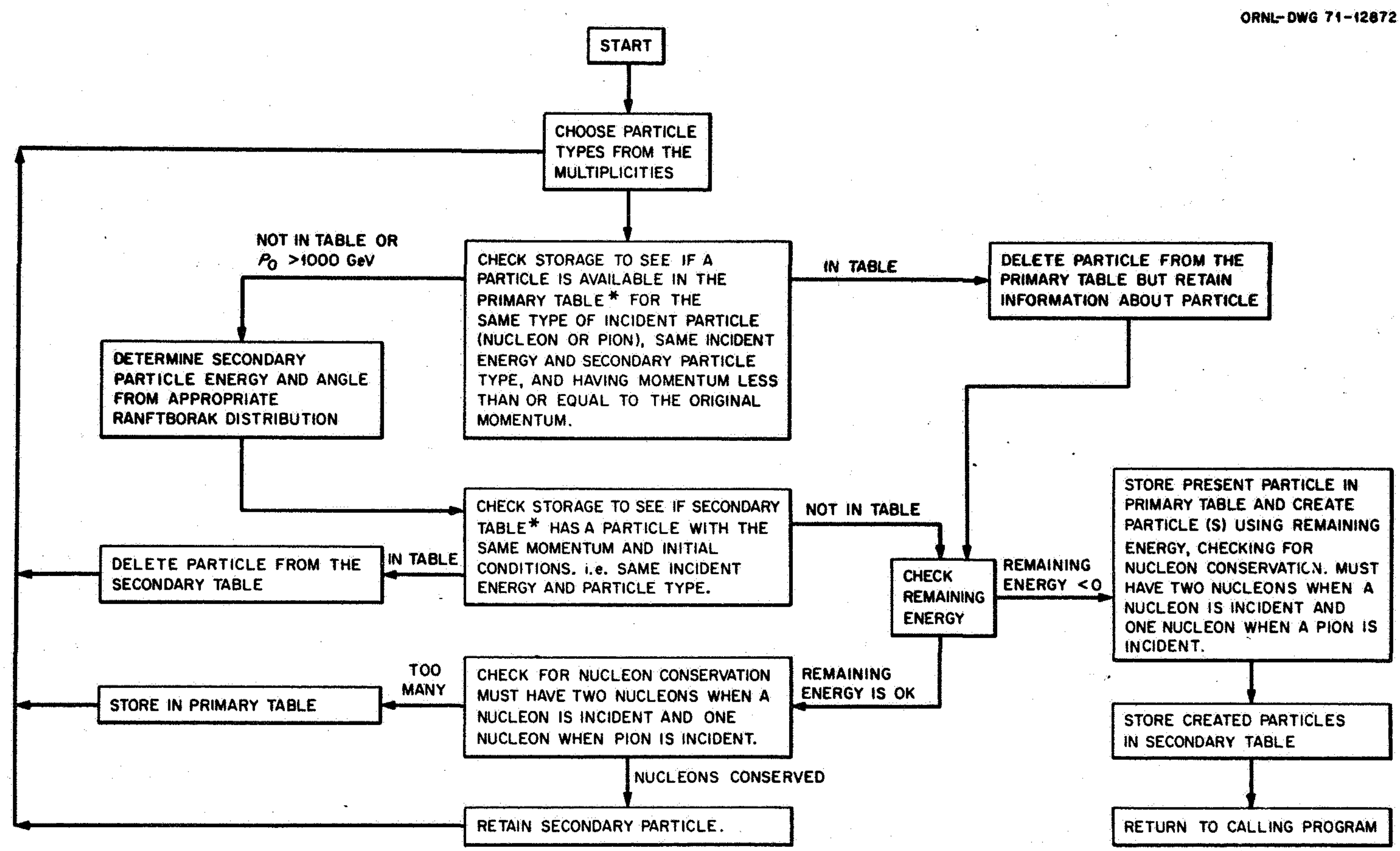

* THE EXACT MOMENTA OF THE PARTICLES THAT ARE CREATED BY SAMPLING (PRIMARY TABLE) AND SECONDARIES THAT ARE CREATED WITHOUT SAMPLING (SECONDARY TABLE) ARE NOT STORED. COUNTERS ARE USED TO REGISTER PARTICLES WITH MOMENTUM ΔP ABOUT P PRODUCED BY INCIDENT NUCLEONS AND PIONS WITH MOMENTUM ΔP_{INC} ABOUT P_{INC}.

Fig. 13. Logic Diagram of the Calculational Procedure.

REFERENCES

1. K. C. Chandler and T. W. Armstrong, "Operating Instructions for the High-Energy Transport Code, HETC," ORNL-4744 (in press).

2. T. A. Gabriel and R. T. Santoro, "Calculation of the Long-Lived Activity in Soil Produced by 500-GeV Protons," ORNL-TM-3262 (1970).

3. V. S. Barashenkov, "Interaction Cross Sections of Elementary Particles," translated from Russian by Y. Oren, Dept. of Physics, Tel Avev University, Israel Program for Scientific Translation, Jerusalem (1968).

4. H. W. Bertini _et al._, "Intranuclear Cascade Calculation of the Secondary Nucleon Spectra From Nucleon-Nucleus Interactions in the Energy Range 340 to 2900 MeV and Comparisons with Experiment," ORNL-TM-2361 (1969).

5. H. W. Bertini, private communication, 1971.

6. B. G. Gibbard _et al._, Phys. Rev. Letters **24**, 22 (1970).

7. J. Ranft and T. Borak, "Improved Nucleon-Meson Cascade Calculations," National Accelerator Laboratory Report FN-193, 1100.0 (1969).

8. G. Trilling, UCID **10**, 148 (1966).

9. S. J. Lindenbaum and R. M. Sternheimer, Phys. Rev. **105**, 1870 (1957).

INTERNAL DISTRIBUTION

1-3. L. S. Abbott
4. F. S. Alsmiller
5. R. G. Alsmiller, Jr.
6. T. W. Armstrong
7-11. J. Barish
12. H. W. Bertini
13. A. A. Brooks
14. H. P. Carter
15. C. E. Clifford
16-35. T. A. Gabriel
36. M. P. Guthrie
37. W. E. Kinney
38. T. A. Love
39. F. C. Maienschein
40. R. W. Peelle
41. R. W. Roussin
42-51. R. T. Santoro
52. D. Sundberg
53. J. A. Turner
54. J. W. Wachter
55. G. E. Whitesides
56. H. A. Wright
57. W. Zobel
58. H. Feshbach (consultant)
59. H. Goldstein (consultant)
60. C. R. Mehl (consultant)
61. H. T. Motz (consultant)
62-63. Central Research Library
64. ORNL·Y-12 Technical Library, Document Reference Section
65-66. Laboratory Records Department
67. Laboratory Records ORNL RC
68. ORNL Patent Office

EXTERNAL DISTRIBUTION

69. P. B. Hemmig, Division of Reactor Development & Technology, U. S. Atomic Energy Commission, Washington, D. C. 20545
70. W. H. Hannum, Division of Reactor Development & Technology, U. S. Atomic Energy Commission, Washington, D. C. 20545
71. Kermit O. Laughon, AEC Site Representative
72. C. V. L. Smith, Physics & Math Branch, Division of Research, U. S. Atomic Energy Commission, Washington, D. C. 20545
73-202. Given AEC High-Energy Accelerator Shielding and NASA Space Shielding Distribution
203-204. Division of Technical Information (DTIE)
205. Laboratory and University Division (ORO)